Korean Membrane Journal
Vol. 8, No. 1 December, 2006, 21-30

# Separation of $CO_2$ and $N_2$ with a NaY Zeolite Membrane under Various Permeation Test Conditions

**Churl Hee Cho**[†], **Jeong Gu Yeo, Young Soo Ahn, Moon Hee Han, and Sang Hoon Hyun**[*]

Functional Materials Research Center, Korea Institute of Energy Research, Daejeon 305-343, Korea
[*]Department of Ceramic Engineering, Yonsei University, Seoul 120-749, Korea

*(Received October 10, 2006, Accepted December 4, 2006)*

Abstract: A faujasite NaY zeolite membrane was prepared on a tubular $\alpha$-$Al_2O_3$ support by the secondary growth process, and effects of permeation test conditions on the $CO_2/N_2$ separation were investigated. A NaY zeolite membrane with good $CO_2/N_2$ separation was successfully synthesized by using the hydrothermal solution ($Al_2O_3$:$SiO_2$:$Na_2O$:$H_2O$ = 1:6:14:840 in a molar base): at a permeation temperature of 30°C, its $CO_2$ permeance and $CO_2/N_2$ separation factor were $2.5 \times 10^{-7}$ mol/m$^2$secPa and 34, respectively. The $CO_2$ and $N_2$ permeations were highly dependent on permeation test conditions (feed composition, feeding rate, feed pressure, He sweeping rate and permeation temperature). The results indicated that (i) $CO_2$ and $N_2$ permeations through NaY zeolite membrane are governed by surface and micropore diffusions, respectively, (ii) the preparation of NaY zeolite membrane with a large permeating area is one of the most difficult hurdles for its real applications, and (iii) the retardation of $N_2$ permeation is an effective key to improve $CO_2/N_2$ separation factor in NaY zeolite membrane.

*Keywords*: NaY zeolite membrane, $CO_2/N_2$ separation, permeation test conditions, surface diffusion, micropore diffusion

## 1. Introduction

Since Kyoto protocol in 1997, researches for carbon dioxide recovery in combustion flue gases have been activated. Carbon dioxide recovery using a membrane has been attended due to its potential applications to recover high purity carbon dioxide with low processing cost. Because carbon dioxide membrane should operate in chemically and thermally severe conditions and call for a high $CO_2$ permeance, an inorganic membrane is more favorable than a polymeric membrane.

Many inorganic materials have been considered as carbon dioxide membranes. Among them, templated silica[1,2], molecular sieving carbon[3-6] and nanoporous zeolite[7-10] membranes are representative and show promising performances on carbon dioxide separation. Verweij and coworkers reported $CO_2$ and $N_2$ permeations through templated silica membranes in single component systems[1]. The templated silica membranes were prepared by calcining dip-coated silica sol films on $\gamma$-$Al_2O_3$-modified $\alpha$-$Al_2O_3$ supports. The templated silica membrane with a $CO_2$ permeance of $2.28\times10^{-7}$ mol/m$^2$secPa and a $CO_2/N_2$ perm-selectivity of 22.8 at 25°C showed a degraded perm-selectivity of 8.6 at 200°C. Fuertes and coworkers prepared molecular sieving carbon membranes by carbonizing spin-coated phenolic resin films on carbon discs, and then investigated $CO_2/N_2$ separations as a function of permeation temperature[3]. In case of the carbon membrane with a $CO_2$ permeance of $5\times10^{-8}$ mol/m$^2$secPa and a $CO_2/N_2$ separation factor of 45 at room temperature, separation factor degraded up to 8, when permeation temperature increased to 150°C. Kusakabe and coworkers synthesized NaY zeolite membranes on $\alpha$-$Al_2O_3$ supports by hydrothermal process, and then in-

---

[†]Author for all correspondences
(e-mail : chcho@kier.re.kr)

vestigated $CO_2/N_2$ separations[7-10]. $CO_2/N_2$ separations of NaY zeolite membranes were promising: at a permeation temperature range of 30~40°C, $CO_2$ permeance and $CO_2/N_2$ separation factor were reported to be up to $1.5\times10^{-6}$ mol/$m^2$secPa and 30, respectively. In some NaY zeolite membranes, separation factor reached up to around 100 at 30°C. But, the promising separation factor rapidly dropped up to 4, as permeation temperature increased to 150°C. In the above-mentioned inorganic membranes, there is an apparent trade-off between separation factor and permeance, and also is an overall trend of decreasing separation factor with increasing permeation temperature. Especially, it is remarkable that NaY zeolite membrane shows not only good $CO_2/N_2$ separation factor but also excellent $CO_2$ permeance.

In a gas separation system using a membrane, its gas recovery rate is directly related to the gas flux permeating through membrane. Gas flux through a membrane is dependent on both membrane-intrinsic permeation properties and system-operational variables. Therefore, in the present study, influences of permeation test conditions (feed composition, feeding rate, feed pressure, He sweeping rate and permeation temperature) on $CO_2/N_2$ separation through NaY zeolite membrane were investigated. From the investigations, $CO_2$ and $N_2$ permeation mechanisms and pre-requirements for its real applications to carbon dioxide recovery process will be discussed.

## 2. Experimental Procedure

### 2.1. Preparation and Materials Characterization of NaY Zeolite Membrane

An $\alpha$-$Al_2O_3$ tube (Ceracom Co., Ltd., Korea) with a length of 50 mm was used as a membrane support. Its outer diameter and thickness were 10 and 1.5 mm, respectively. The $\alpha$-$Al_2O_3$ support was cleaned by 3 times acetone washings and then calcination at 500°C for 4 hours. Its porosity and mean pore diameter were analyzed by a mercury porosimeter. Particulate NaY zeolites with an average diameter of 230 nm were seeded on the outer surface of the $\alpha$-$Al_2O_3$ support using a vacuum-assisted filtering system. The non-seeded and seeded $\alpha$-$Al_2O_3$ supports were dried and reserved at 110°C, and then applied to the following membrane preparation process.

NaY zeolite membranes were deposited on the outer surface of the $\alpha$-$Al_2O_3$ support by hydrothermal process. Aqueous hydrothermal solutions were made of water glass (Cat. No. 193-08185, Wako Pure Chemical Industries, Ltd., Japan), sodium aluminate (Cat. No. 1923-3260, Showa Chemicals Inc., Japan) and sodium hydroxide (Cat. No. 39155-0350, Junsei Chemical Co., Ltd., Japan), and then aged at room temperature for 24 hours. The final composition of aqueous hydrothermal solution was $Al_2O_3:SiO_2:Na_2O:H_2O$ = 0.1-1:2-20:6-22: 840 in a molar basis. An $\alpha$-$Al_2O_3$ support was vertically installed with a teflon-made zig in a polyprophylene bottle with a volume of 125 mL, where a 100 mL of hydrothermal solution was introduced. The $\alpha$-$Al_2O_3$ support was hydrothermally treated in the aqueous hydrothermal solution at 80~120°C for 4~72 hours. Zeolite crystals grew on the surface of the $\alpha$-$Al_2O_3$ support under hydrothermal condition. After the hydrothermal process, a prepared zeolite membrane was 3 times washed with clean water by repeated filtration and stirring processes, until the pH value of washing water dropped up to 8, and then stored in a desiccator with particulate silica dehumidifiers.

Crystalline phase and morphology of zeolite membranes were analyzed by X-ray diffractometer (D/max 2000-Ultima$^{Plus}$ Rigaku, Japan) and scanning electron microscopy (XL30, Philips, Holland), respectively. In the morphology observations using SEM, the molar ratio of Si to Al in zeolite membrane was evaluated by EDS analysis.

### 2.2. Evaluation of Gas Permeation Property of NaY Zeolite Membranes

Carbon dioxide and nitrogen permeations through NaY zeolite membrane were evaluated for single and binary gases. First, a prepared NaY zeolite membrane

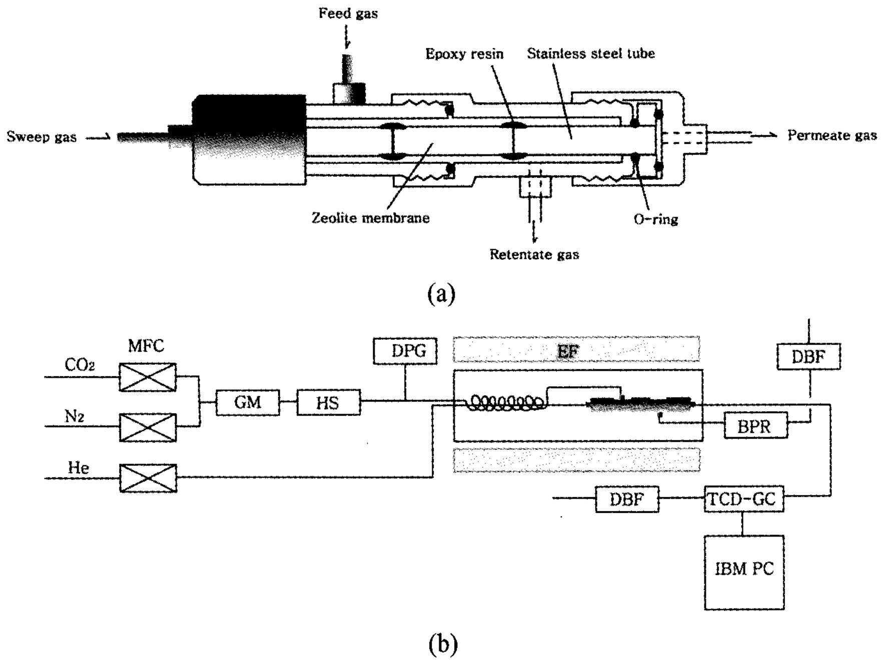

**Fig. 1.** Schemes: (a) membrane test cell and (b) permeation test system.

was installed in a membrane test cell. Before the membrane installation, two stainless steel tubes with an outer diameter of 10 mm were attached on each side with an epoxy resin. Schemes for the membrane test cell and permeation test system used in the present study were represented in Figs. 1(a) and (b), respectively. Feed composition, feeding rate and He sweeping rate were controlled by mass flow controllers (MFCs). Permeation temperature was controlled by an electric furnace (EF) where the membrane test cell shown in Fig. 1(a) was installed in. Single or binary gas goes through a gas mixer (GM) and a humidity scrubber (HS) to feed side. Feed pressure was controlled by a back pressure regulator (BPR), installed in retentate side.

Generally, gas permeation through a membrane is represented by its permeance or flux, and selectivity.

Permeance means how fast a component permeates through a membrane. Permeance of *i* component is defined as moles of *i* component permeating through unit permeating area of a membrane for unit time per unit pressure, and is represented as the following equation:

$$\Pi(i) = \frac{J(i)}{p(i)_f - P(i)_p} \qquad (1)$$

where $\Pi(i)$ is the permeance of *i* component (moles/$m^2$secPa), $J(i)$ is the flux of *i* component (moles/$m^2$sec), $p(i)$ is the partial pressure of *i* component (Pascal), and subscripts *f* and *p* represent feed and permeate sides, respectively. In the present study, $CO_2$ and $N_2$ fluxes were calculated from the flow rate of permeate gas, the room temperature, the molar ratio of $CO_2$ to $N_2$ in permeate side, and the permeating area of membrane. The flow rate of permeate gas was measured by a digital bubble flow meter (DBF). The molar ratio of $CO_2$ to $N_2$ in permeate side was measured by a TCD-GC (ACME 6000, Young Lin Co., Ltd, Korea). The permeating area of a membrane was calculated by its outer diameter and length. Feed pressure was measured by a digital pressure gauge (DPG). $CO_2$ and $N_2$ permeances were calculated from the $CO_2$ and $N_2$ fluxes, the molar ratio of $CO_2$ to $N_2$ in feed side, and the feed pressure. The three following assumptions were applied to the permeance calculations in $CO_2$-$N_2$ binary component system: (i) the temperature of permeate gas introduced to the digital bubble flow meter (DBF) doesn't be affected by furnace temperature and is equal to room temperature, (ii) He carrier gas doesn't affect $CO_2$ and $N_2$ permeations through membrane, and (iii) $CO_2$ and $N_2$ partial pressures in permeate side is zero.

Selectivity indicates how much faster a component permeates through a membrane than others. Usually, selectivity is represented by two distinguishable terms: one is perm-selectivity and the other is separation factor. Perm-selectivity is selectivity for single gas and separation factor is one for binary gas.

Perm-selectivity of *i* to *j* components is defined as the ratio of the permeance of pure *i* component to the permeance of pure *j* component as the following equation:

$$F_{\alpha} = \frac{\Pi(i)}{\Pi(j)} \tag{2}$$

where $F_{\alpha}$ is the perm-selectivity of *i* to *j* components, and $\Pi(i)$ and $\Pi(j)$ are the permeances of pure *i* and *j* components, respectively. In the present study, the permeances of pure $CO_2$ and $N_2$ gases were evaluated when feed pressure is 2 bar and He sweeping rate is zero. In the permeance calculations for single gas using equation (1), it was assumed that the partial pressures in feed and permeate sides is 2 and 1 bar, respectively, because feed gas is a pure gas and He sweeping rate was zero.

Separation factor in a binary gas of *i* and *j* components can be calculated from the molar ratios of *i* component to *j* component in feed and permeate sides as the following equation:

$$\alpha = \frac{(x/y)_p}{(x/y)_f} \tag{3}$$

where $\alpha$ is the separation factor of *i* to *j* components, and *x* and *y* represent the mole fractions of *i* and *j* components, respectively. In the present study, $CO_2$ and $N_2$ mole fractions in permeate and feed sides were calculated from the molar ratio of $CO_2$ to $N_2$ in permeate and feed sides, measured by the TCD-GC.

## 3. Results and Discussion

### 3.1. Preparation and Materials Characteristics of NaY Zeolite Membranes

NaY zeolite membranes were prepared by heterogeneous growth of NaY zeolite crystals on the outer surface of the tubular $\alpha$-$Al_2O_3$ support under hydrothermal conditions. The influences of hydrothermal conditions (presence of seed layer, heating and cooling schedules, and composition of hydrothermal solution) on the heterogeneous growth were investigated. In the present study, any defect-free NaY zeolite membrane wasn't prepared on a non-seeded $\alpha$-$Al_2O_3$ support under a wide range of hydrothermal condition. On the other hand, defect-free NaY zeolite membranes were reliably synthesized on the outer surface of the seeded $\alpha$-$Al_2O_3$ support under a special range of hydrothermal condition. NaY zeolite membranes with high $CO_2/N_2$ separation factor were successfully prepared by hydro-thermally treating seeded $\alpha$-$Al_2O_3$ supports at 110°C for 24 hours in aqueous solutions of which composition was $Al_2O_3$:$SiO_2$:$Na_2O$:$H_2O$=1:6:14:840 in a molar basis. The optimum synthesis condition for NaY zeolite preparation was so different from ones reported by others[7-14].

Figs. 2(a) to (f) represent SEM images for surfaces and cross-sections of a tubular $\alpha$-$Al_2O_3$ support, a seeded $\alpha$-$Al_2O_3$ support and a zeolite membrane prepared under the optimum synthesis condition. The tubular $\alpha$-$Al_2O_3$ support was very porous: its average porosity and mean pore diameter were 35 vol.% and 0.12 μm, respectively. In the seeded $\alpha$-$Al_2O_3$ support, there was a well-developed thin layer of seeds. In the prepared zeolite membrane, zeolite crystals were uniformly deposited on the outer surface of the $\alpha$-$Al_2O_3$ support and its average thickness was around 5 μm.

Fig. 3 represents X-ray diffraction (XRD) patterns of (a) a tubular $\alpha$-$Al_2O_3$ support, (b) particulate NaY seeds,

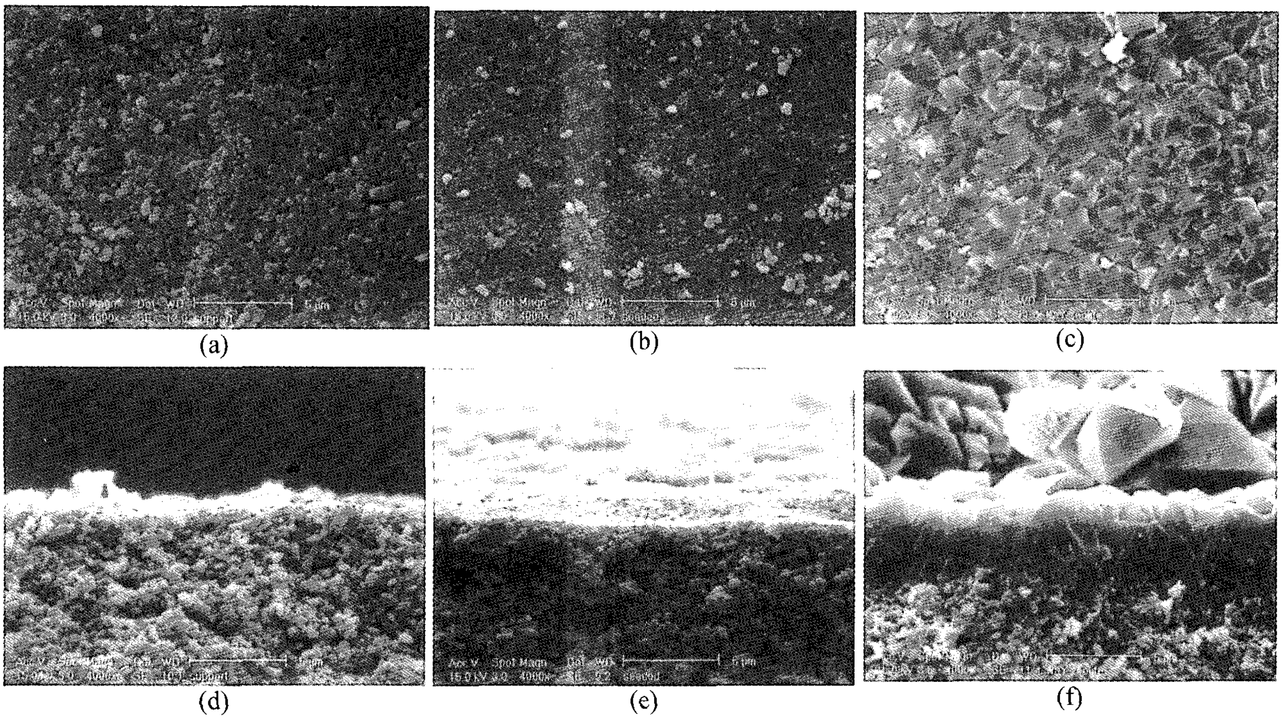

**Fig. 2.** SEM images for surfaces and cross-sections of a tubular $\alpha$-$Al_2O_3$ support, a seeded $\alpha$-$Al_2O_3$ support and a prepared zeolite membrane. Figs. 2(a) to (c) are images for surfaces and Figs. 2(d) to (f) are ones for cross-sections.

(c) a seeded $\alpha$-$Al_2O_3$ support and (d) a zeolite membrane prepared under the optimum synthesis condition. The $\alpha$-$Al_2O_3$ support showed typical XRD peaks for $\alpha$-$Al_2O_3$ phase and seeds did ones for NaY zeolite phase. In the XRD pattern of the seeded $\alpha$-$Al_2O_3$ support, a trace of NaY zeolite phase was shown, but its intensity was ignorable. On the other hand, XRD pattern for the prepared zeolite membrane was clearly composed of XRD peaks for both $\alpha$-$Al_2O_3$ and faujasite zeolite phases. The zeolite crystals grown on the outer surface of the seeded $\alpha$-$Al_2O_3$ support were faujasite-type zeolite crystals. In the composition analysis using EDS, the atomic ratio of Si to Al in the faujasite zeolite membrane was 1.68. The grown zeolite crystals were faujasite NaY zeolite crystals.

### 3.2. Gas Permeation Through NaY Zeolite Membranes

Kusakabe and coworkers have made extensive studies of the $CO_2/N_2$ separation of NaY zeolite membrane [7-10]. According to their report[8], the NaY zeolite membrane with atomic Si/Al ratio of 1.54 showed a good $CO_2/N_2$ separation performance: at a permeation temperature of 40°C, its $CO_2/N_2$ separation factor was around 30 and its $CO_2$ permeance was about $1 \times 10^{-6}$ $mol/m^2secPa$. Also, their remarkable findings could be summarized by the following sentences: (i) the high $CO_2/N_2$ separation factor for binary gas is caused by the selective adsorption of $CO_2$ molecules, because $CO_2$ molecules adsorbed on the pore walls effectively prevent non-adsorptive $N_2$ molecules from penetrating through NaY zeolite membrane[7], (ii) $CO_2$ and $N_2$ permeations through NaY zeolite membrane can be explained by an adsorption-diffusion model, in which total flux of a gas is a summation of fluxes due to surface diffusion and Knudsen flow[9]. If $CO_2$ and $N_2$ fluxes are dominated by surface diffusion and Knudsen flow, respectively, their expressions for $CO_2$ and $N_2$ fluxes can be simplified as the following equations, when $CO_2$ and $N_2$ partial pressures in permeate side are zero:

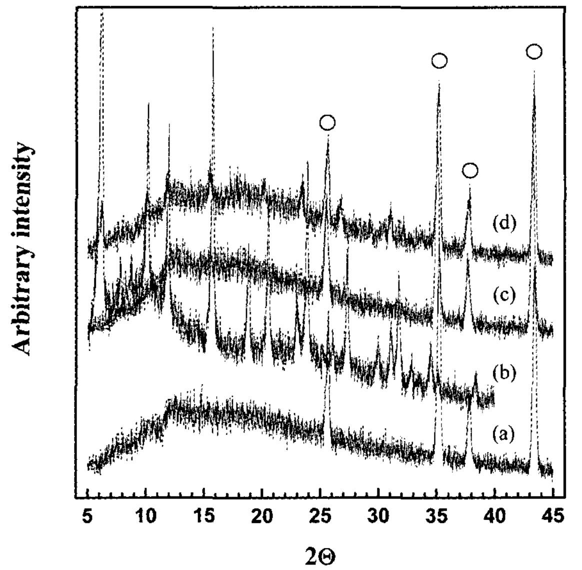

**Fig. 3.** XRD patterns: (a) tubular $\alpha$-$Al_2O_3$ support, (b) particulate NaY seeds, (c) seeded $\alpha$-$Al_2O_3$ support and (d) NaY zeolite membrane. Open circles indicate XRD peaks for $\alpha$-$Al_2O_3$ phase and others are ones for faujasite zeolite.

$$J(CO_2) \approx a\ln[1+bp(CO_2)_f] \tag{4}$$

$$J(N_2) \approx cp(N_2)_f \tag{5}$$

where a, b and c are temperature-dependent constants.

Generally, permeation mechanism of a gas through a membrane is elucidated by studying effects of permeation test conditions (feed pressure, permeation temperature, and so on) on flux or permeance of a gas permeating through a membrane. In the present study, effects of feed composition, feeding rate, feed pressure, He sweeping rate and permeation temperature on $CO_2$ and $N_2$ permeations through NaY zeolite membrane were investigated.

Table 1 represents $CO_2$ and $N_2$ fluxes and $CO_2/N_2$ perm-selectivity of NaY zeolite membrane for single $CO_2$ and $N_2$ gases. Feeding rate and feed pressure was 150 mL/min and 2 bar, respectively. He sweeping rate was zero, so that the pressure of single gas in permeate side was 1 bar. With increasing permeation temperature, $CO_2$ flux showed a maximum at a permeation temperature of 80°C and $N_2$ flux continuously increased.

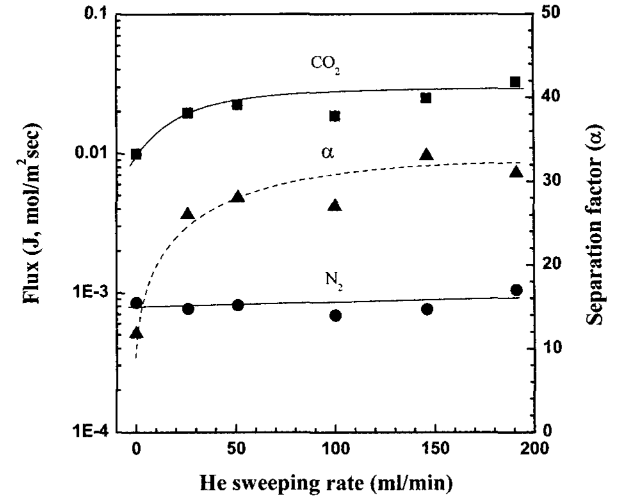

**Fig. 4.** $CO_2$ and $N_2$ fluxes and $CO_2/N_2$ separation factor at 30°C as a function of He sweeping rate.

As the result, $CO_2/N_2$ perm-selectivity decreased with increasing permeation temperature. It was remarkable that $N_2$ flux was two to six times smaller than $CO_2$ flux, but was in the same order of $CO_2$ flux.

Fig. 4 represents $CO_2$ and $N_2$ fluxes and $CO_2/N_2$ separation factor at 30°C as a function of He sweeping rate. Feed gas was an equimolar binary gas of $CO_2$ and $N_2$, and its pressure and feeding rate were 2 bar and 350 mL/min, respectively. As He sweeping rate in permeate side increased, $CO_2$ flux through NaY zeolite membrane increased, whereas $N_2$ flux through NaY zeolite membrane is nearly independent of He sweeping rate. This could be explained by the improved driving force of $CO_2$ flux with increasing He sweeping rate. The increment of He sweeping rate leaded to the decrement of $CO_2$ and $N_2$ partial pressures in permeate side. At higher He sweeping rate, $CO_2$ and $N_2$ molecules adsorbed in permeate side were more easily desorbed. Especially, $CO_2$ molecules with good adsorptive affinity on NaY zeolite were more easily desorbed at larger He sweeping rate, so that $CO_2/N_2$ separation factor increased with increasing He sweeping rate. It was interesting that when He sweeping rate was zero, $CO_2$ and $N_2$ fluxes for binary gas were much smaller than those for single gases represented in Table 1: $CO_2$ flux decreased from $4.54 \times 10^{-2}$ to $1.0 \times 10^{-2}$ and $N_2$

**Table 1.** $CO_2$ and $N_2$ Fluxes and $CO_2/N_2$ Perm-selectivity in Single $CO_2$ and $N_2$ Systems

| Temperature (°C) | Flux ($10^{-2}$ mol/m$^2$sec) | | Perm-selectivity |
|---|---|---|---|
| | $CO_2$ | $N_2$ | $CO_2/N_2$ |
| 30 | 4.54 | 0.75 | 6.1 |
| 50 | 5.16 | 1.39 | 3.7 |
| 80 | 5.26 | 1.85 | 2.8 |
| 100 | 5.06 | 2.23 | 2.3 |

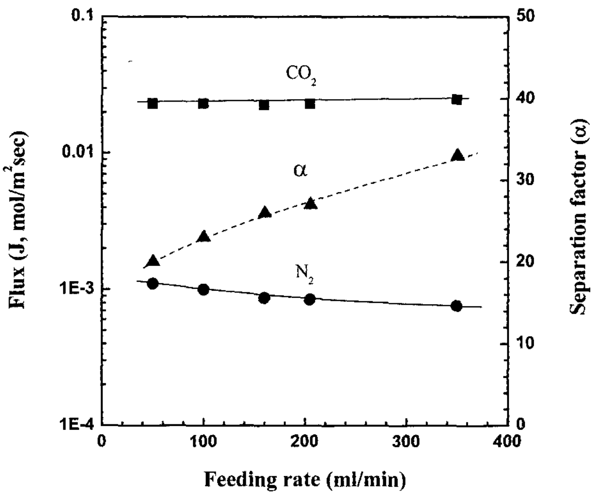

**Fig. 5.** $CO_2$ and $N_2$ fluxes and $CO_2/N_2$ separation factor at 30°C as a function of feeding rate.

flux did from $7.5 \times 10^{-3}$ to $8.5 \times 10^{-4}$ mol/m$^2$sec. This means that $CO_2$ and $N_2$ molecules permeating through NaY zeolite membrane interrupt each other to reduce the flux of counterpart. Especially, $CO_2$ molecule more effectively obstructs the permeation of $N_2$ molecule. Also, it is remarkable that He sweeping significantly improved $CO_2$ flux and $CO_2/N_2$ separation factor. This indicates that in an adsorption-assisted membrane such as NaY zeolite membrane, gas permeation properties measured in a He sweeping mode might be over-estimated, because it is impossible to introduce a sweep gas in real applications.

Fig. 5 represents $CO_2$ and $N_2$ fluxes and $CO_2/N_2$ separation factor at 30°C as a function of feeding rate of an equimolar binary gas. Feed pressure was 2 bar and He sweeping rate was 146 mL/min. As feeding rate increased, $CO_2$ flux was nearly independent of feeding rate, whereas $N_2$ flux a little decreased. Under consideration that feed pressure remains constant, it is reasonable that $CO_2$ and $N_2$ fluxes are nearly independent of feeding rate. However, $N_2$ flux a little decreased with increasing feeding rate. This slight decrement of $N_2$ flux with increasing feeding rate might be related with the slight decrement of feed pressure due to Bernoulli's principle, but its exact origin is still unknown.

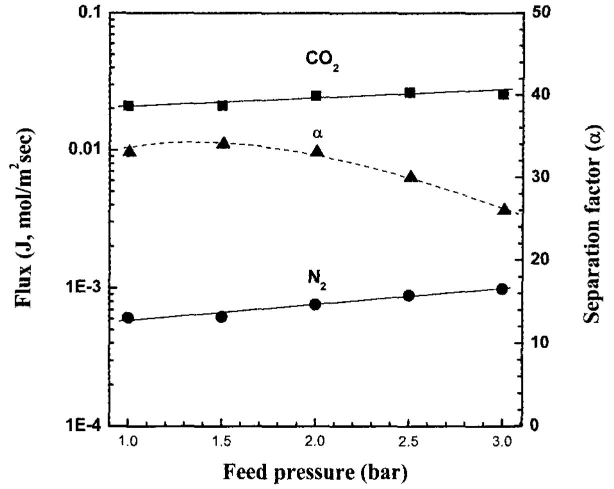

**Fig. 6.** $CO_2$ and $N_2$ fluxes and $CO_2/N_2$ separation factor at 30°C as a function of feed pressure.

Fig. 6 represents $CO_2$ and $N_2$ fluxes and $CO_2/N_2$ separation factor at 30°C as a function of feed pressure. The feeding and He sweeping rates were 350 and 146 mL/min, respectively. As feed pressure increased, $CO_2$ and $N_2$ fluxes a little increased. Relatively, $N_2$ flux showed more gradient increasing behavior than $CO_2$ flux, so that $CO_2/N_2$ separation factor decreased with increasing feed pressure. In Langmuir adsorption theory, an equilibrium adsorption of a gas on a porous adsorbent increases as gas pressure increases[9]. Therefore, the slight increase of $CO_2$ flux with feed pressure originated in the slight increase of equilibrium adsorption, because $CO_2$ partial pressure in feed side increased with increasing feed pressure. As shown in equation (1), the permeance is the flux divided by the difference of partial pressure between feed and permeate sides. If $N_2$ permeation through NaY zeolite membrane was governed by Knudsen flow, $N_2$ permeance should be independent of feed pressure, according to equations (1) and (5). In the present study,

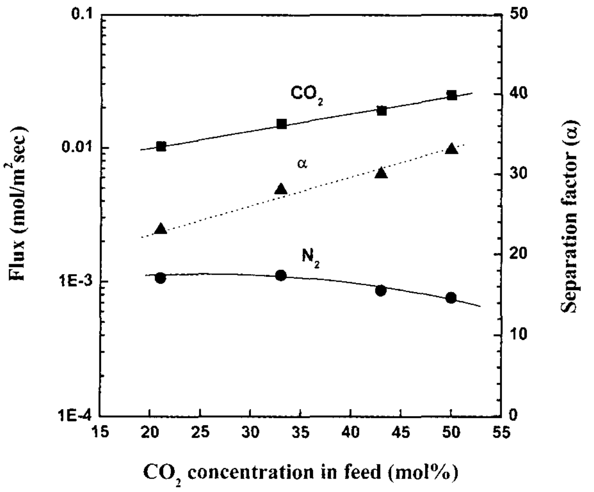

**Fig. 7.** $CO_2$ and $N_2$ fluxes and $CO_2/N_2$ separation factor at 30°C as a function of $CO_2$ concentration in feed gas.

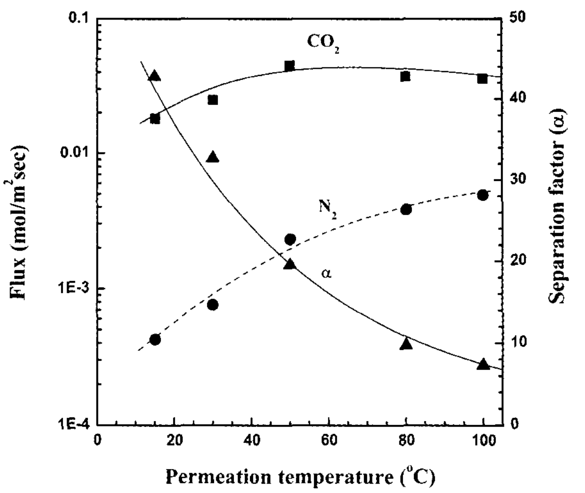

**Fig. 8.** $CO_2$ and $N_2$ fluxes and $CO_2/N_2$ separation factor as a function of permeation temperature.

$N_2$ permeance rapidly decreased as feed pressure increased. This indicates that $N_2$ permeation through NaY zeolite membrane might not be governed by Knudsen flow mechanism at a permeation temperature of 30°C. Kusakabe and coworkers have reported that the high $CO_2/N_2$ separation factor of NaY zeolite membrane stemmed from the effective obstruction of $CO_2$ molecules adsorbed in narrow pores to the penetration of non-adsorptive $N_2$ molecules[7]. The slight increase of equilibrium adsorptions will more effectively prevent $N_2$ molecules from permeating through nanopores in NaY zeolite membrane. Therefore, the improved driving force due to the increase of $N_2$ partial pressure difference will be compensated with the decrease of driving force due to the improved obstruction of adsorbed $CO_2$ molecules. Also, it is remarkable that $CO_2$ flux was nearly independent of feed pressure. This means that the increment of feed pressure doesn't improve $CO_2$ recovery rate in a $CO_2$ separation system using a NaY zeolite membrane, so that it is necessary to prepare NaY zeolite membranes with large permeating area for the improvement of $CO_2$ recovery rate.

Fig. 7 represents $CO_2$ and $N_2$ fluxes and $CO_2/N_2$ separation factor at 30°C as a function of $CO_2$ concentration in feed gas. Feed pressure and He sweeping rate were 2 bar and 146 mL/min. In all cases, feeding rate was more than 200 mL/min. As shown in Fig. 5, the effect of feeding rate on $CO_2$ and $N_2$ fluxes is inconsiderable. As the $CO_2$ concentration in feed gas increased, $CO_2$ flux increased and $N_2$ flux decreased, so that $CO_2/N_2$ separation factor increased with increasing the $CO_2$ concentration in feed gas. This was explained by the increase of $CO_2$ concentration in feed side. As $CO_2$ concentration in feed gas increases, $CO_2$ equilibrium adsorption in feed side increases, so that $N_2$ penetration through NaY zeolite membrane gets more difficult. Therefore, $CO_2/N_2$ separation factor increases with increasing $CO_2$ concentration in feed gas.

Fig. 8 represents $CO_2$ and $N_2$ fluxes and $CO_2/N_2$ separation factor as a function of permeation temperature. Feed gas was an equimolar binary gas of $CO_2$ and $N_2$, and its pressure and feeding rate were 2 bar and 350 mL/min, respectively. He sweeping rate was 146 mL/min. As permeation temperature increased, $CO_2$ flux increased up to $4.5 \times 10^{-2}$ mol/m$^2$sec at 50°C and then decreased. On the other hand, $N_2$ flux continuously increased with increasing permeation temperature. Kusakabe and coworkers have reported similar results and then explained by the degraded $CO_2$ adsorptive affinity and the improved $CO_2$ surface diffusivity with increasing permeation temperature[9]. If $N_2$ permeation through NaY zeolite membrane is governed by Knudsen flow, $N_2$ flux must decrease with increasing permeation temperature[15]. But in the present study, $N_2$ flux continuously increased as permeation temperature increased. This again indicates that $N_2$ permeation through NaY zeolite membrane is governed by micropore diffusion rather than Knudsen flow, at permeation temperatures of less than 100°C. Therefore, to improve $CO_2/N_2$ separation factor, it is necessary to effectively retard $N_2$ permeation through NaY zeolite membrane.

## 4. Conclusions

NaY zeolite membranes were successfully formed on a tubular $\alpha$-$Al_2O_3$ support and the influences of permeation test conditions on $CO_2/N_2$ separation behavior were investigated. From the results, as-followings were known.

1) Carbon dioxide and nitrogen permeations through NaY zeolite membrane were governed by surface diffusion and micropore diffusion mechanisms, respectively, at permeation temperatures of less than 100°C.

2) Feed pressure made little effect on $CO_2$ flux, so that it is the most important factor to reliably prepare NaY zeolite membrane with a large permeating area in its real applications to separation processes.

3. $CO_2/N_2$ separation factor decreased as permeation temperature increased. Therefore, to improve separation factor at elevated temperatures, it is necessary to develop a technique to retard $N_2$ permeation through NaY zeolite membrane at elevated temperatures.

## Acknowledgements

This research was supported by a grant (DB2-201) from Carbon Dioxide Reduction & Sequestration Research Center, one of the $21^{st}$ Century Frontier Programs funded by the Ministry of Science and Technology of Korean government.

## References

1. R. M. de Vos and H. Verweji, Improved performance of silica membranes for gas separation, *J. Membr. Sci.*, **143**, 37 (1998).
2. R. M. de Vos, W. F. Maier, and H. Verweji, Hydrophobic silica membranes for gas separation, *J. Membr. Sci.*, **158**, 277 (1999).
3. T. A. Centeno and A. B. Fuertes, Supported carbon molecular sieve membranes based on a phenolic resin, *J. Membr. Sci.*, **160**, 201 (1999).
4. T. A. Centeno and A. B. Fuertes, Carbon molecular sieve membranes derived from a phenolic resin supported on porous ceramic tubes, *Sep. Purif. Technol.*, **25**, 379 (2001).
5. H. B. Park and Y. M. Lee, Pyrolytic carbon-silica membrane: a promising membrane materials for improved gas separation *J. Membr. Sci.*, **213**, 263 (2003).
6. H. B. Park, Y. K. Kim, J. M. Lee, S. Y. Lee, and Y. M. Lee, Relationship between chemical structure of aromatic polyimides and gas permeation properties of their carbon molecular sieve membrane, *J. Membr. Sci.*, **229**, 117 (2004).
7. K. Kusakabe, T. Kuroda, A. Murate, and S. Morooka, Formation of a Y-type zeolite membranes on a porous $\alpha$-alumina tube for gas separation, *Ind. Eng. Chem. Res.*, **36(3)**, 649 (1997).
8. K. Kusakabe, T. Kuroda, and S. Morrooka, Separation of carbon dioxide from nitrogen using ion-exchanged faujasite-type zeolite membranes formed on porous support tubes, *J. Membr. Sci.*, **148**, 13 (1998).
9. Y. Hasegawa, K. Kusakabe, and S. Morooka, Effect of temperature on the gas permeation properties of NaY-type zeolite formed on the inner surface of a porous support tube, *Chem. Eng. Sci.*, **56**, 4273 (2001).
10. K. Kusakabe, T. Kuroda, K. Uchino, Y. Hasegawa, and S. Morooka, Gas permeation properties of ion-exchanged faujasite-type zeplite membranes, *AIChE J.*, **45(6)**, 1220 (1999).
11. H. Kita, T. Inoue, H. Asamura, K. Tanaka, and K. Okamoto, NaY zeolite membrane for the pervapo-

ration separation of methanol-methyl *tert*-butyl ether mixtures, *Chem. Commun.* 45 (1997).

12. H. Kita, K. Fuchida, T. Horita, H. Asamura, and K. Okamoto, Preparation of faujasite membranes and their permeation properties, *Sep. Purif. Technol.*, **25**, 261 (2001).
13. M. Lassinantti, J. Hedlund, and J. Sterte, Faujasite-type films synthesizing by seeding, *Micropor. Mesopor. Mater.*, **38**, 25 (2000).
14. K. Weh, M. Moack, I. Sieber, and J. Caro, Permeation of single gaes and gas mixtures through faujasite-type molecular sieve membranes, *Micropor. Mesopor. Mater.*, **54**, 27 (2002).
15. S. V. Sotrichos and V. N. Burganos, *MRS Bulletin* **24(3)**, 41 (1999).